Electronic Supplementary Information

Amphiphile Self-Assembly Dynamics at the Solution-Solid Interface Reveal Asymmetry in Head/Tail Desorption

Henry D. Castillo[a]†, John M. Espinosa-Duran[a]†, James R. Dobscha[a], Daniel C. Ashley[a,b], Sibali Debnath[a], Brandon E. Hirsch[a,c], Samantha R. Schrecke[a,d], Mu-Hyun Baik[a,e], Peter J. Ortoleva[a], Krishnan Raghavachari[a], Amar H. Flood[a], Steven L. Tait[a]*

[a.] *Department of Chemistry, Indiana University, 800 E. Kirkwood Avenue, Bloomington, Indiana 47405, USA*
[b.] *Current address: Department of Chemistry, North Carolina State University, Raleigh, North Carolina 27695, USA*
[c.] *Current address: Division of Molecular Imaging and Photonics, Department of Chemistry, KU Leuven–University of Leuven Celestijnenlaan 200F, 3001 Leuven (Belgium)*
[d.] *Current address: Department of Chemistry, Texas A&M University, College Station, Texas 77840, USA*
[e.] *Current address: Department of Chemistry, Korea Advanced Institute of Science and Technology 291 Daehak-ro, Yuseong-gu Daejeon, 34141, Republic of Korea*
† These authors contributed equally to this work.
* Corresponding author: tait@indiana.edu, Tel.: +1-812-855-1302

Experimental

General Synthetic Methods

All reagents were obtained from commercial suppliers and were used as received unless otherwise noted. NMR spectra were recorded on Varian Inova (400 and 500 MHz) and Varian VXR (400 MHz) at room temperature (298 K). Chemical shifts were referenced to residual solvent peaks. The series of alkoxybenzonitrile molecules have been previously reported[1-3] and were prepared according to a modified literature procedure.[3]

4-(Octadecyloxy)benzonitrile (ABN-C_{18}) – 4-Hydroxybenzonitrile (0.5 g, 4.2 mmol), 1-bromooctadecane (1.33 g, 4 mmol), and K_2CO_3 (1.74 g, 12.6 mmol) was dissolved in acetonitrile (50 ml) and heated to reflux overnight. After cooling to room temperature, water was added, and the mixture was extracted with EtOAc. The organic layer was dried with $MgSO_4$, filtered, and dried in vacuo to give compound **ABN-C_{18}** as a waxy white solid. (1.15 g, 3.15 mmol, 75% yield) **ABN-C_{18}** was used without further purification. ^{1}H NMR (400 MHz, chloroform-*d*) δ / ppm = 7.57 – 7.49 (m, 2H), 6.93 – 6.85 (m, 2H), 3.96 (t, *J* = 6.6 Hz, 2H), 1.77 (p, *J* = 6.8 Hz, 2H), 1.41 (q, *J* = 7.6 Hz, 2H), 1.38 – 1.25 (m, 4H), 1.25 (s, 4H), 1.23 (s, 19H), 0.85 (t, J = 6.8 Hz, 3H). ^{13}C NMR (100 MHz, chloroform-*d*) δ / ppm = 162.41, 133.86, 119.23, 115.12, 103.60, 77.35, 77.04, 76.72, 68.38, 31.91, 29.69, 29.65, 29.56, 29.52, 29.35, 29.30, 28.96, 25.91, 22.67, 14.09.

4-(Hexadecyloxy)benzonitrile (ABN-C_{16}) – Compound **ABN-C_{16}** was prepared as a pure white solid following the same procedure as **ABN-C_{18}** in 82% yield from 4-hydroxybenzonitrile and 1-bromohexadecane. **ABN-C_{16}** was used without further purification. ^{1}H NMR (400 MHz, chloroform-*d*) δ / ppm = 7.55 (d, *J* = 8.8 Hz, 2H), 6.91 (d, *J* = 8.8 Hz, 2H), 3.97 (t, *J* = 6.5 Hz, 2H), 3.39 (t, *J* = 6.9 Hz, 0H), 1.79 (tt, *J* = 14.2, 7.1 Hz, 2H), 1.47 – 1.38 (m, 2H), 1.42 – 1.26 (m, 3H), 1.25 (d, *J* = 6.7 Hz, 22H), 0.86 (t, *J* = 6.7 Hz, 3H). ^{13}C NMR (100 MHz, chloroform-*d*) δ / ppm = 162.41, 133.90, 119.29, 115.12, 103.59, 68.38, 34.03, 32.82, 31.89, 29.65, 29.63, 29.61, 29.54, 29.50, 29.41, 29.33, 29.28, 28.94, 28.74, 28.15, 25.89, 22.66, 14.09.

4-(Dodecyloxy)benzonitrile (ABN-C_{12}) – Compound **ABN-C_{12}** was prepared as a pure white solid following the same procedure as **ABN-C_{18}** in 80% yield from 4-hydroxybenzonitrile and 1-bromododecane. **ABN-C_{12}** was used without further purification. ^{1}H NMR (400 MHz, chloroform-*d*) δ / ppm = 7.59 – 7.49 (m, 2H), 6.95 – 6.85 (m, 2H), 3.97 (t, *J* = 6.5 Hz, 2H), 1.83 – 1.71 (m, 2H), 1.49 – 1.37 (m, 2H), 1.33 (d, *J* = 6.5 Hz, 1H), 1.25 (d, *J* = 7.4 Hz, 14H), 0.86 (t, *J* = 6.7 Hz, 3H). ^{13}C NMR (100 MHz, chloroform-*d*) δ / ppm = 162.42, 133.91, 115.13, 103.58, 68.39, 31.88, 29.61, 29.59, 29.53, 29.50, 29.31, 29.28, 28.94, 25.89, 22.65, 22.29, 14.09.

4-(Octyloxy)benzonitrile (ABN-C$_8$) – Compound **ABN-C$_8$** was prepared as a clear viscous oil following the same procedure as **ABN-C$_{18}$** in 82% yield from 4-hydroxybenzonitrile and 1-bromooctane. **ABN-C$_8$** was used without further purification. 1H NMR (400 MHz, chloroform-*d*) δ / ppm = 7.59 – 7.50 (m, 2H), 6.95 – 6.86 (m, 2H), 3.97 (t, J = 6.5 Hz, 2H), 1.83 – 1.71 (m, 2H), 1.49 – 1.37 (m, 2H), 1.39 – 1.21 (m, 8H), 0.91 – 0.82 (m, 3H). ^{13}C NMR (100 MHz, chloroform-*d*) δ / ppm = 162.42, 133.90, 119.30, 115.13, 103.58, 68.39, 56.85, 31.75, 29.24, 29.16, 28.94, 27.05, 25.90, 22.61, 14.06.

4-(Butyloxy)benzonitrile (ABN-C$_4$) – Compound **ABN-C$_4$** was prepared as a clear viscous oil following the same procedure as **ABN-C$_{18}$** in 85% yield from 4-hydroxybenzonitrile and 1-bromobutane. **ABN-C$_4$** was used without further purification. ^{1}H NMR (400 MHz, chloroform-*d*) δ / ppm = 7.59 – 7.50 (m, 2H), 6.94 – 6.87 (m, 2H), 3.98 (t, J = 6.5 Hz, 1H), 1.76 (dq, J = 7.9, 6.5 Hz, 2H), 1.48 (dt, J = 14.9, 7.4 Hz, 2H), 0.96 (t, J = 7.4 Hz, 3H). ^{13}C NMR (100 MHz, chloroform-*d*) δ / ppm = 162.42, 133.90, 119.30, 115.13, 103.58, 68.06, 30.96, 22.29, 19.11, 13.74.

General Methods for Scanning Tunneling Microscopy

STM experiments were carried out on Agilent Technologies 5500 PicoPlus STM using a Picoscan 1.18.1 controller in constant-current mode. Tips were mechanically cut from Pt/Ir wire (80:20, 0.25 mm diameter). Voltage pulses between 2 to 10 V with 1 to 3 ms duration were occasionally conducted to improve image quality. Unless noted, all experiments were conducted at room temperature.

Samples were prepared by dropping 2 µL of solution via micropipette onto a freshly cleaved HOPG surface (ZYB, 10 × 10 × 1 mm). HOPG was mechanically cleaved using scotch tape, and a minor circular impression was made in the HOPG surface by pressing a viton o-ring on the surface for several seconds. The impression prevented the liquid sample from wicking off the HOPG surface. Solutions were prepared with either octanoic acid (≥ 99%), hexanoic acid (≥ 99%), or 1:3 mixture (by volume) of dodecanoic acid (≥ 99%) and 1-phenyloctane (98%). Typical scanning parameters ranged from I_t = 0.03 to 0.2 nA, V_{sample} = -0.6 to -1.2 V.

All high-resolution STM images were corrected for drift effects and piezo scanner calibration by comparison to lattice measurements of the underlying HOPG (recorded by using scan conditions different from those used to measure molecular assemblies (I_t = 0.1 to 0.2 nA, V_{sample} = -0.002 to -0.005 V). Unit-cell measurements (including angles relative to the HOPG lattice) were acquired after correcting the high-resolution images and averaging the distances.

Force Field Parameters

Different CHARMM-compatible force fields were tested in the simulations. All-atom force fields (FFs) were used to model the steric orientations of atoms in the alkyl chains and HOPG. FFs for alkoxybenzonitriles and octanoic acid were generated using AFMM (Automated Frequency Matching Method)[4] with CHARMM (Chemistry at HARvard Molecular Mechanics).[5] The initial parameters to be fitted were obtained from Swissparam[6] and CGenFF[7]. These unoptimized constructed FFs were initially tested, yielding very good results (~12% error) for the unit cell measurements when compared to the experimentally known values. However, in order to improve the accuracy of the predictions, these FFs were optimized for the alkoxybenzonitriles and for octanoic acid. In these FFs, all the bonded parameters were optimized using B3LYP[8-12] 6-31+G(d)[13] and charges were from ESP-fitted charges (**Figure S1**). The force constants for different parameter were fitted in such a way to obtain a good correlation between MM and QM vibrational frequencies. Quantum mechanical calculations for FF parametrization were performed in Jaguar.[14]

To assess the quality of the bonded parameters of the FF, the QM vibrational frequencies were compared to the MM frequencies. Vibrational frequencies were in excellent agreement with an average correlation of R^2=0.99 (**Figure S2a** and **b**). To evaluate the quality of the non-bonded parameters, the density from MD simulations at 1 atm @ 300K was compared to the experimentally measured density. Experimental and simulated densities were in excellent agreement with a correlation of R^2=0.923 (**Figure S2c**). It should be noted that the Lennard Jones parameters for alkoxybenzonitriles and octanoic acid were taken from Charmm 22/CMAP.[15]

For HOPG, the atom positions were fixed and no charges were assigned to the atoms. No intramolecular or intermolecular interactions were considered within HOPG, and HOPG only interacts with the adsorbates through vdW forces. The parameters were taken from the CA atom type in CHARMM 22/CMAP. No image charge or induced dipole interactions were allowed.

The MD simulation results presented here were obtained using such FF.

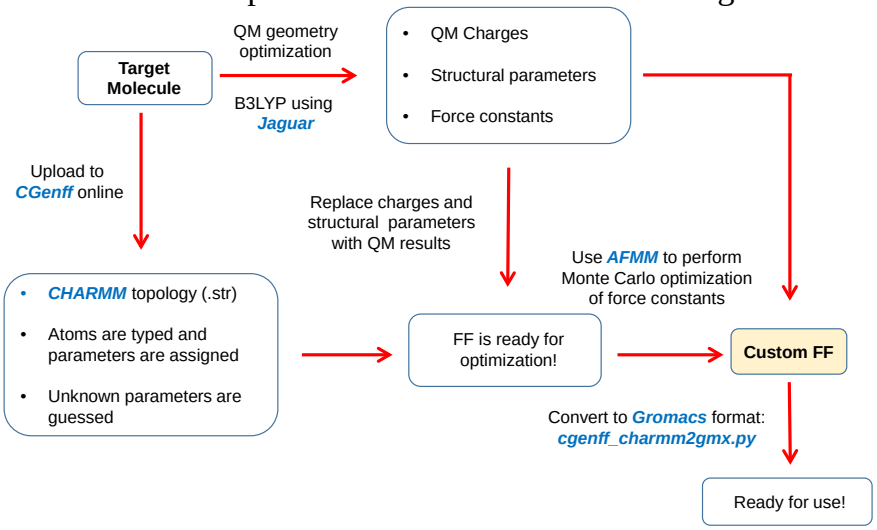

Figure S1. Flow diagram of the algorithm used for the generation of the custom FF for the alkoxybenzonitriles and octanoic acid.

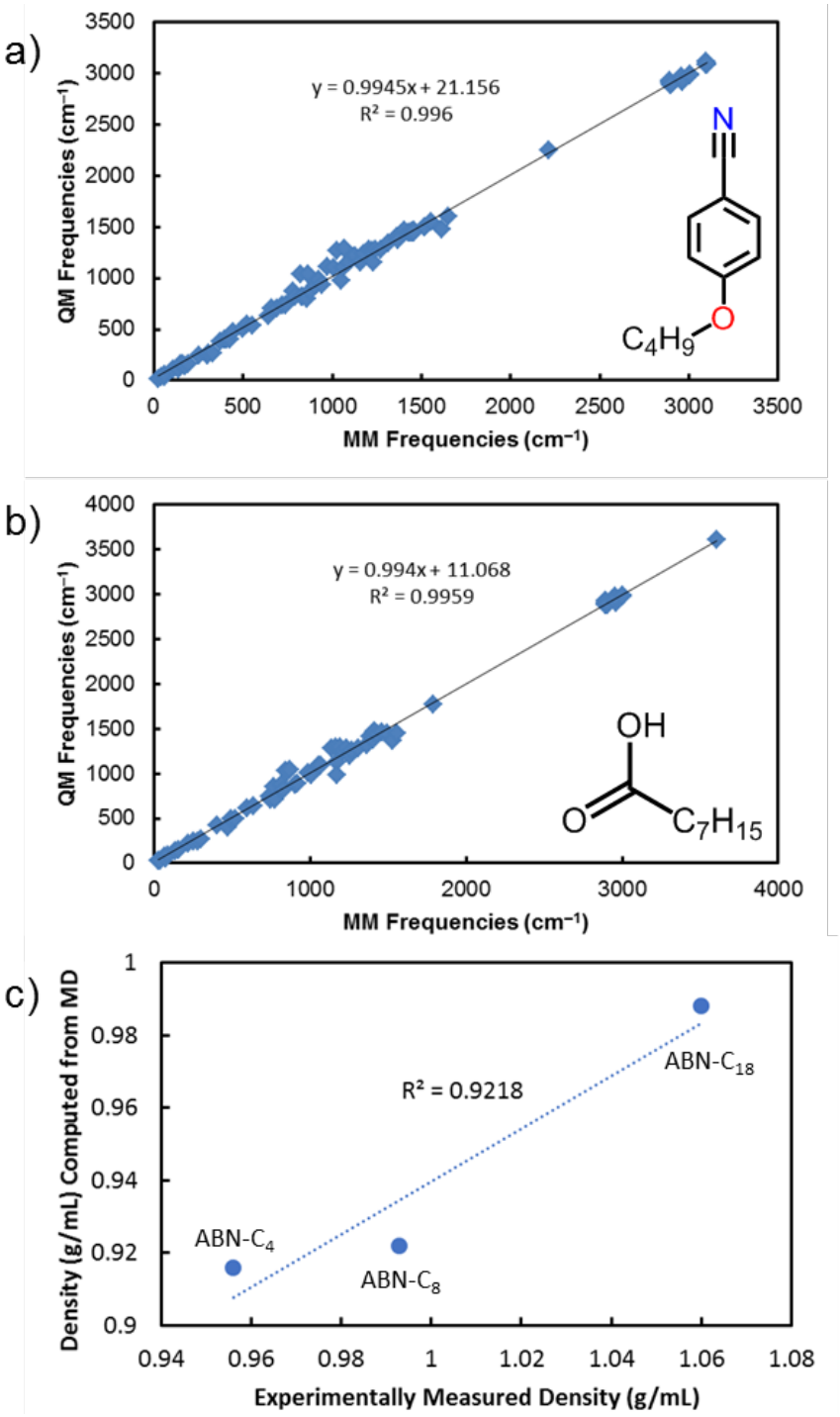

Figure S2. Correlation between QM frequencies and MM frequencies given the customized FF for (a) **ABN-C$_4$** and (b) octanoic acid. (c) Correlation between the densities (g/ml) measured experimentally and computed from MD simulations for alkoxybenzonitriles with customized FF.

Systems Design and Preparation

HOPG was simulated as four layers of AB stacked graphene, each one 13 nm x 23 nm (~1800 nm^3). As an approximation to speed up simulations, the position of the carbon atoms in HOPG were fixed. The all-atom structure of the alkoxybenzonitrile molecule was optimized in Gaussian09[16] using B3LYP-D3/6-31+G(d).[13, 17-19] MD Simulations were performed considering two different initial states for the alkoxybenzonitriles absorbed on HOPG: random molecular orientations, and ordered interdigitated tails (meso-scale order) with unit cell dimensions taken from STM data (**Figure S3**). Initially random orientations simulated the beginning stages of self-assembly in which molecules are adsorbed, but not ordered on the HOPG surface. The initially ordered orientations simulated a more developed state in which small domains are already formed. The very initial stages of adsorption and self-assembly, in which molecules start from a solvated state away from the surface and then adsorb onto HOPG, were not simulated. Preliminary simulations of **ABN-C_{18}** at an initially solvated state (not in contact with the surface) were attempted, but molecules remained in solution and failed to adsorb even after 100 ns. Thus, solvated initial states were not simulated.

Hundreds of alkoxybenzonitriles molecules were included in each simulation to achieve almost full coverage of the graphite surface, from 360 **ABN-C_4** to 152 **ABN-C_{18}**; this implies that the molecular density increases for molecules with shorter tail length. The simulations were performed in vacuum (no solvent) in octanoic acid as solvent. A pre-equilibrated (300 K @ 1 atm) solvent box with 1700-1900 octanoic acid molecules was prepared and then added to the simulation box to fill all the simulation volume up to 3 nm on top of the absorbed molecules. A different system was prepared for each one of the four alkoxybenzonitrile molecules, each solvent condition and each initial organization, for a total of 16 systems. For simulations with octanoic acid, the concentrations of **ABN-C_{18}**, **ABN-C_{12}**, **ABN-C_8**, **ABN-C_4** are respectively 233 mM, 286 mM, 414 mM, and 444 mM.

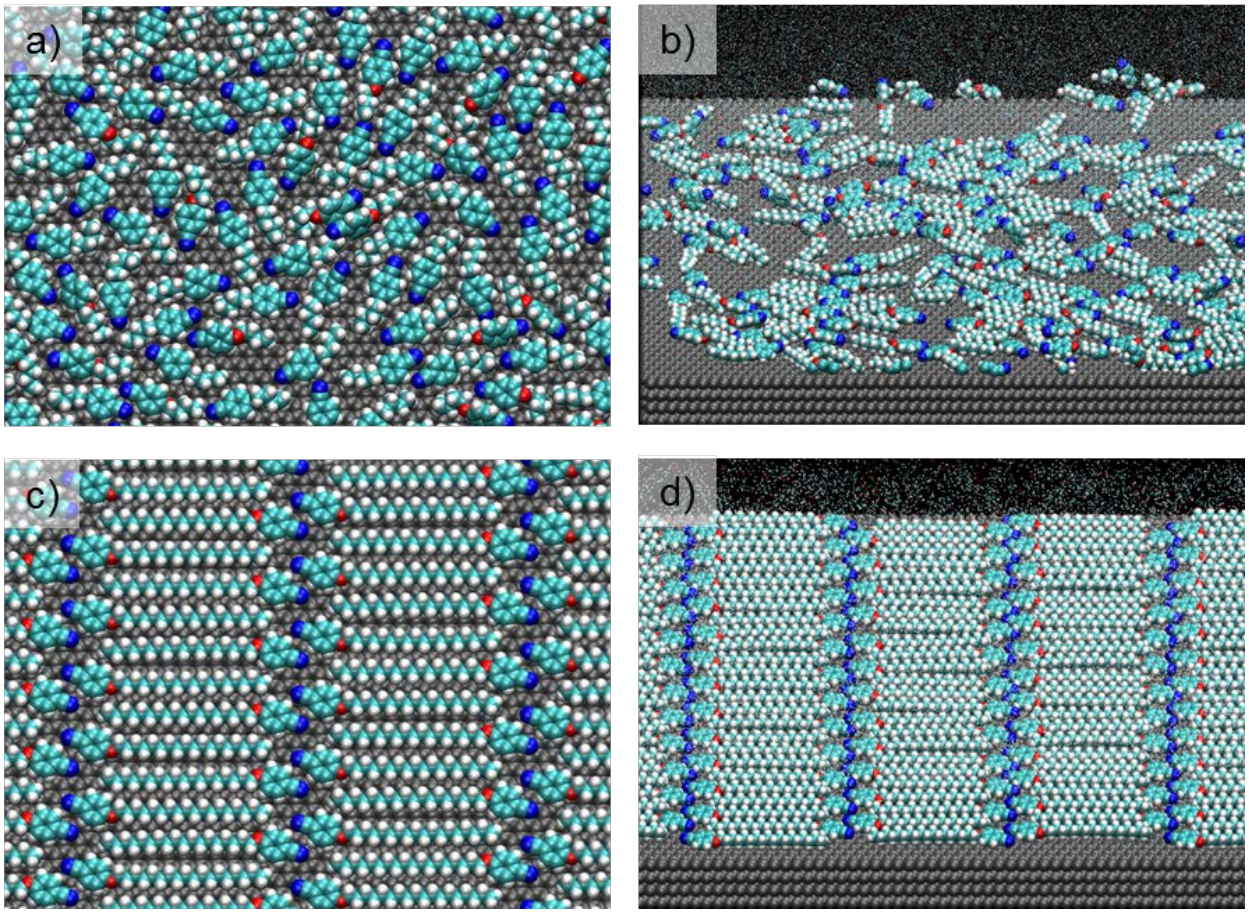

Figure S3. Initial configurations of alkoxybenzonitrile molecules for MD simulations. Initially disordered: (a) **ABN-C$_4$**, and (b) **ABN-C$_8$**; initially ordered: (c-d) **ABN-C$_{18}$**.

Simulation Conditions

Each simulation was performed for at least 200 ns under room temperature conditions (300 K) using an NVT ensemble and containing only one type of alkoxybenzonitrile. The simulation of initially random molecules allows the visualization of dynamic molecular processes that lead to assembly of alkoxybenzonitriles into ordered structures with atomic resolution. The simulation of initially interdigitated (ordered) molecules allows to predict the stability of the structures. Since the 2C crystalline structure has not been resolved for **ABN-C$_4$**, the unit cell values of **ABN-C$_8$** were used by shortening the larger dimension.

Then, the systems were energy minimized individually using steepest descent and then conjugate gradient algorithms. This was followed by 1 ns NVT simulation at 300 K using V-rescale thermostat[20] to thermalize the system. The production runs were performed under NVT conditions using a Nose-Hoover thermostat[21] set to 300 K. For all simulation stages, VdW interactions were calculated with a 2.0 nm cut-off radius; Coulomb interactions were calculated using the Reaction-Field-Zero method[22] with a 2.0 nm cut-off radius, and the neighbor list has a radius of 2.3 nm. The cut-off scheme used was group, hydrogen bonds were constrained using the LINCS algorithm,[23] and long range dispersion corrections for the energy were applied. Periodic Boundary Conditions (PBC) were applied in the xy directions, and a wall was imposed in the z direction. The simulations were performed in Gromacs 4.6.5.[24]

Simulation Analysis

Analysis of nanoscale motions was conducted in VMD[25] and was automated through algorithms which were directly run in the VMD console. Data processing was conducted in MATLAB.[26] Distances were measured with respect to the center of the atoms. Desorbed molecules were defined as having all atoms greater than or equal to 5 Å from the top-most graphene sheet. Partial desorption of alkyl chains was defined as any carbon atom in the alkyl chain having a distance greater than or equal to 5 Å from the nearest atom in the top-most graphene sheet. Partial desorption of benzonitrile group was defined as any carbon or nitrogen atom in the benzonitrile group having a distance greater than or equal to 5 Å from the nearest atom in the top-most graphene sheet.

Supplemental Experimental Results

Unit Cells of Alkoxybenzonitriles

Table S1. Unit cell measurements and surface densities for alkoxybenzonitriles with different alkyl chain length obtained from STM (top) and MD simulations (bottom). Unit cell dimensions *a*, *b*, and *γ* are defined in **Fig. 2b** and are reported as averages of multiple measurements with ± 1 standard deviation. *α* is the angle between the *a* vector of the unit cell and the closest major axis of HOPG.

Unit Cells from STM Measurements

	ABN-C$_{18}$	**ABN-C$_{16}$**	**ABN-C$_{12}$**	**ABN-C$_8$**	**ABN-C$_4$** [5]
a (Å)[1]	9.9 (± 0.3)	10.3 (± 1.5)	9.6 (± 0.7)	11.8	---
b (Å)[1]	35.3 (± 0.9)	28.5 (± 3.8)	27.1 (± 1.2)	21.2 (± 0.6)	---
γ (Degrees)[1]	95.0 (± 4.0)	99.1 (± 5.3)	96.7 (± 6.8)	103 (± 2.9)	---
Density (ABN/nm^2)[2]	0.57 (± 0.02)	0.69 (± 0.13)	0.77 (± 0.07)	0.82	---
α (Degrees)[4]	29	---	29	---	---

Unit Cells from MD Simulations

	ABN-C$_{18}$	**ABN-C$_{16}$** [6]	**ABN-C$_{12}$**	**ABN-C$_8$**	**ABN-C$_4$**
a (Å)[3]	9.3 (± 0.4)	---	9.7 (± 0.4)	9.6 (± 0.5)	9.9 (± 0.3)
b (Å)[3]	33.9 (± 2.3)	---	25.2 (± 0.9)	20.2 (± 1.1)	14.6 (± 0.3)
γ (Degrees)[3]	96.7 (± 6.5)	---	95.0 (± 6.9)	93.0 (± 10)	97.8 (± 2.8)
Density (ABN/nm^2)[2]	0.63 (± 0.05)	---	0.82 (± 0.04)	1.03 (± 0.08)	1.38 (± 0.05)
α (Degrees)[3]	24.4 (± 1.1)	---	12.6 (± 3.2)	18.5 (± 7.0)	24.5 (± 1.1)

[1] Obtained by averaging unit cells measurements from 20-25 STM images of each species at various concentrations.
[2] Calculated from unit cell dimensions.
[3] Obtained by averaging 15-30 unit cells measured in the last frame of the MD simulation. Unit cell measurements from MD simulations were obtained from simulations with an ordered initial state after 368 ns (**ABN-C$_{18}$**), 285 ns (**ABN-C$_{12}$**), 368 ns (**ABN-C$_8$**), or 362 ns (**ABN-C$_4$**).
[4] Measured from images with atomic resolution of HOPG lattice in same image as ABN rows. Measured for **ABN-C$_{18}$** and **ABN-C$_{12}$** only.
[5] No interdigitated phase for **ABN-C$_4$** was observed in STM experiments.
[6] **ABN-C$_{16}$** was not simulated with MD.

STM Images of Adsorbed Layers of Solvents: Octanoic Acid and Dodecanoic Acid

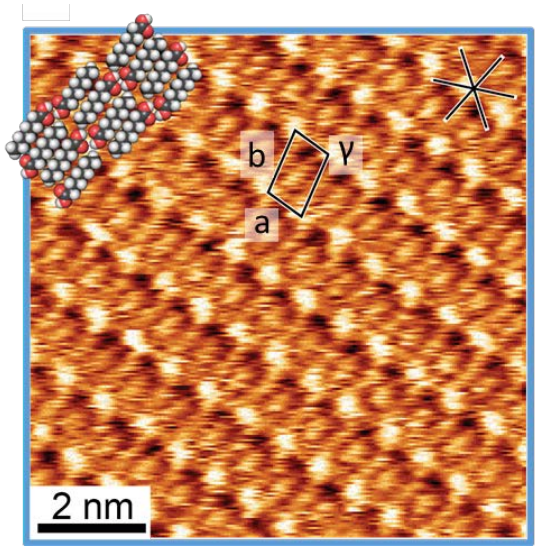

a (Å)	8.7 (± 0.7)
b (Å)	14.5 (± 1.1)
γ (Degrees)	110 (± 5.7)

Figure S4. STM image of octanoic acid self-assembly with molecular model overlay and unit cell dimensions. Conditions: I_t = 0.23 nA, V_{sample} = −0.95 V.

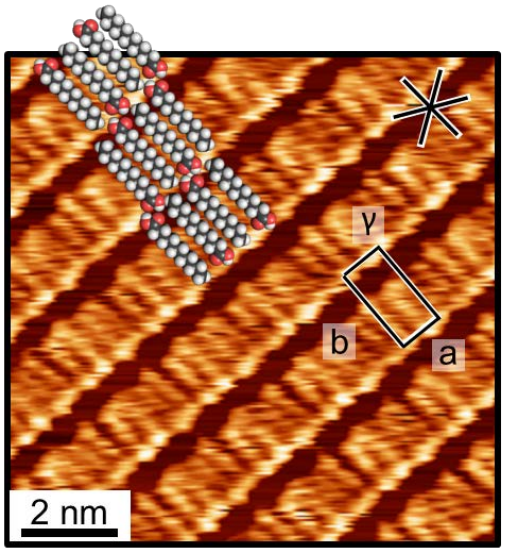

a (Å)	10.2 (± 1.0)
b (Å)	18.8 (± 0.4)
γ (Degrees)	102 (± 7.2)

Figure S5. STM image of dodecanoic acid self-assembly with molecular model overlay and unit cell dimensions. Conditions: I_t = 0.06 nA, V_{sample} = −0.80 V.

MD Simulations of Alkoxybenzonitriles from Two Different Initial States

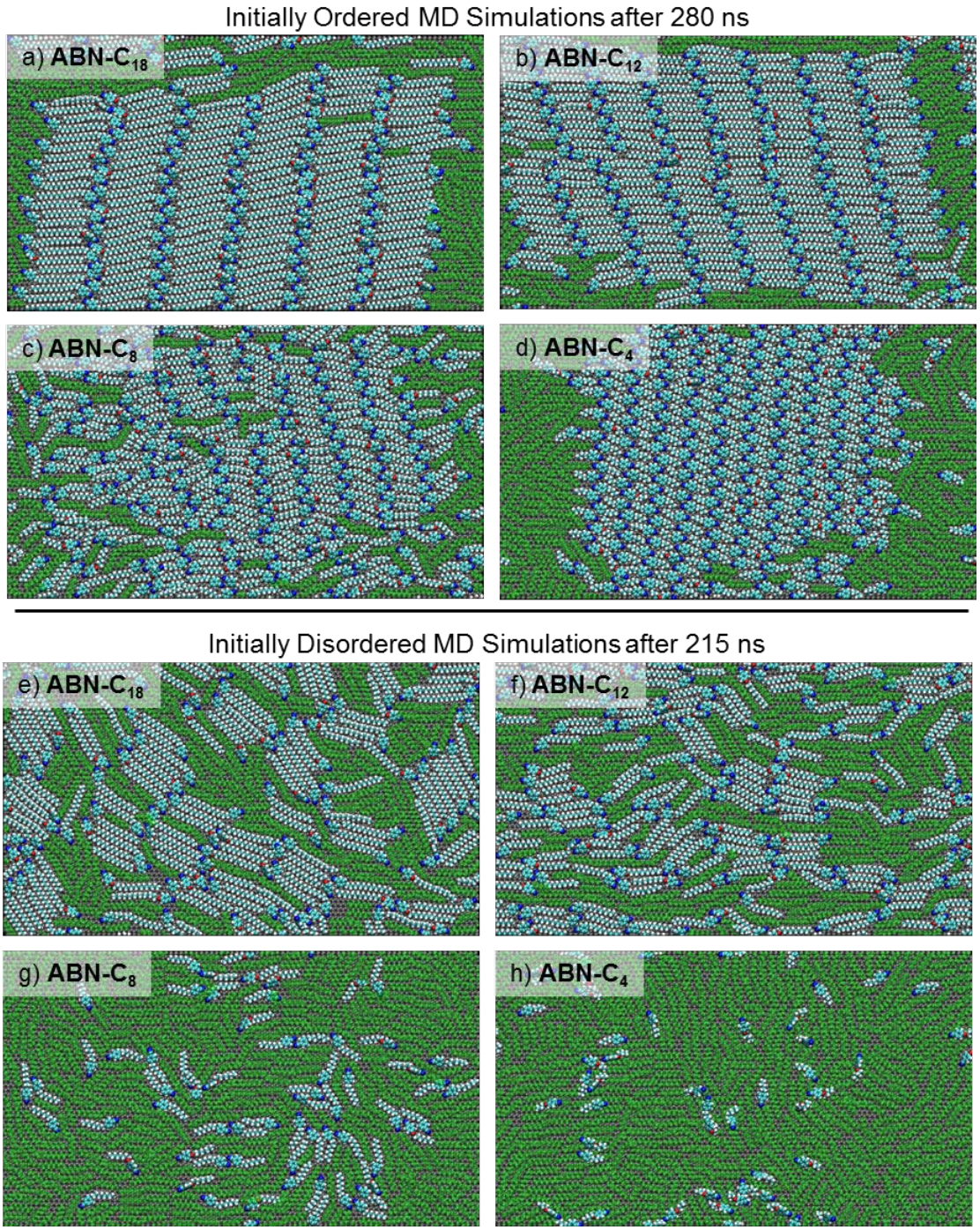

Figure S6. (a-d) MD simulations from initially ordered states of alkoxybenzonitriles with varying chain length at 280 ns. (e-h) MD simulations from initially disordered states of alkoxybenzonitriles with varying chain length at 215 ns. Adsorbed octanoic acid is represented in green. Desorbed alkoxybenzonitrile and octanoic acid molecules have been omitted for clarity.

DFT Calculations of Alkoxybenzonitrile Interactions

Gas-phase QM calculation were performed on alkoxybenzonitriles to estimate the strength of the intermolecular interactions. To compute inter-adsorbate interactions, non-bonded dimers of alkoxybenzonitriles were assembled and potential energy scans were performed using B3LYP D3/6-311++G(d,p) to obtain the energies and distances for the most stable dimers. To compute the interaction energy of alkoxybenzonitriles with HOPG, the adsorption energy was computed using DFT-B with dispersion correction by using a graphene nanoribbon with the alkoxybenzonitrile at the centre. Geometrical optimization of the dimers was not preformed because it bends the molecules.[27] Bending would be incorrect in this case, since the molecules should remain flat as they are absorbed on HOPG. For the benzonitrile dimer interactions, the nitrogen-nitrogen ideal separation is found to be 4.3 Å, with an energy of 5.1 kcal/mol, and for alkyl chains of **ABN-C$_{12}$**, **ABN-C$_8$**, and **ABN-C$_6$**, the carbon-to-carbon ideal separation between antiparallel tails is found to be 4.9 Å. All distance measurements match structures observed with STM. The interaction energies between two alkyl chains are 6.3 kcal/mol, 4.4 kcal/mol and 3.35 kcal/mol for **ABN-C$_{12}$**, **ABN-C$_8$**, and **ABN-C$_6$**, respectively. **Fig. S6** shows a plot of the energies with respect to the alkyl chain length, and the slope is 0.525 kcal/mol-per-carbon, in agreement with DFT-D calculations for pure alkanes that indicate a value of 0.53 kcal/mol-per-carbon).[28] The respective adsorption energies for **ABN-C$_{12}$**, **ABN-C$_8$**, and **ABN-C$_6$** are 5.8, 4.9 and 4.4 kcal/mol. However, considering that the interdigitated organization involves alkyl chains interacting with two neighbouring chains, the strength of the tail-to-tail interaction doubles to 12.6 kcal/mol, 8.8 kcal/mol and 6.7 kcal/mol for **ABN-C$_{12}$**, **ABN-C$_8$**, and **ABN-C$_6$**, respectively. Thus, vdW interactions between alkyl chains dominate adsorbate-adsorbate interactions for **ABN-C$_8$** through **ABN-C$_{18}$**.

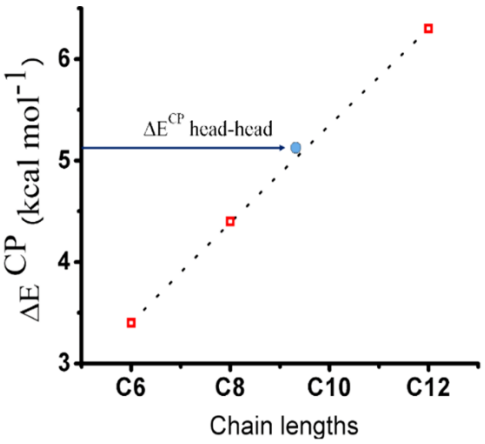

Figure S7. Tail-to-tail interaction energy (with counterpoise correction, CP) between dimers of alkoxybenzonitrile molecules as a function of chain length. The head-to-head interaction is shown for reference over the trend-line (gas phase, B3LYP D3/6-311++G(d,p)).

Alignment of Alkoxybenzonitirles with Graphite Lattice from MD Simulations

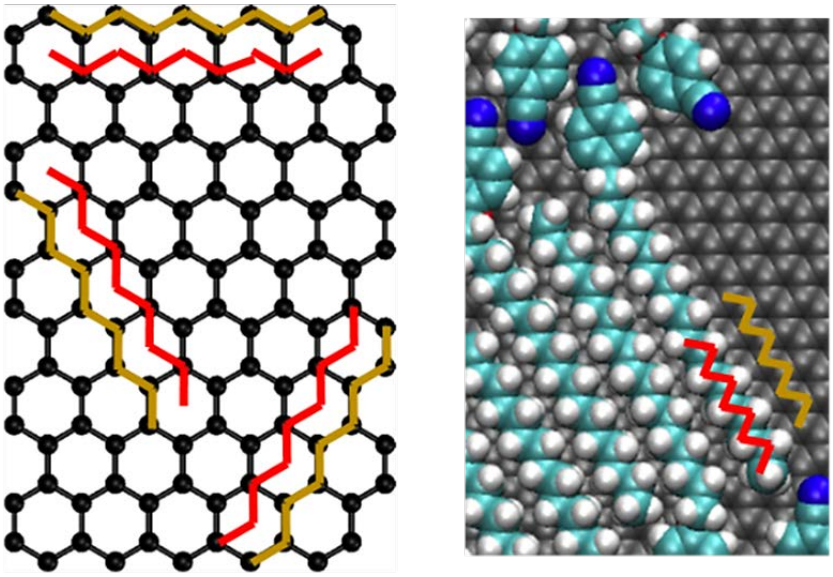

Figure S8. (Left) Graphite lattice; the red lines indicate the preferred orientation of alkyl chains on graphite. (Right) Commensurate orientation of **ABN-C$_{18}$** alkyl chains with the graphite lattice in MD simulations.

CH•••NC Bond Angle and Distance Distribution from Initially Ordered MD Simulations

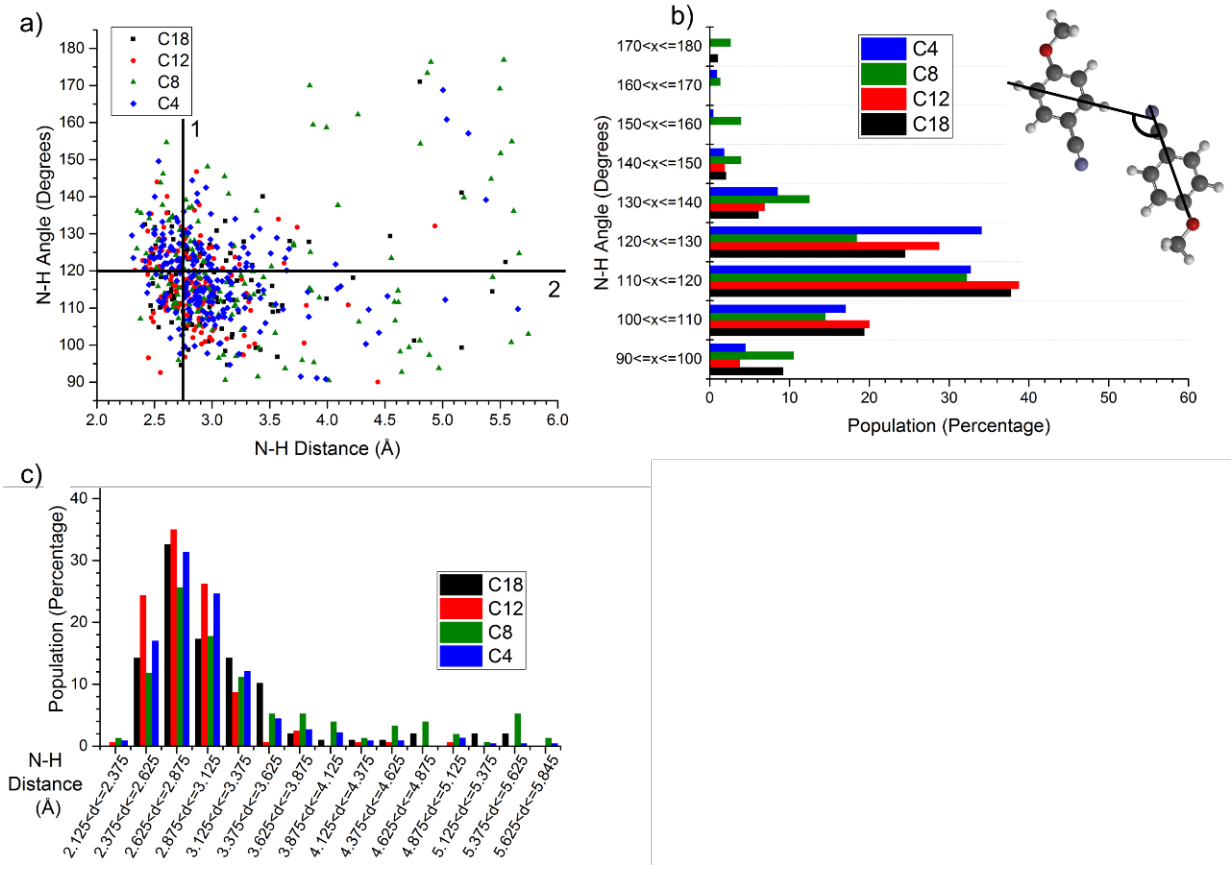

Figure S9. (a) Hydrogen bond angle vs. distance between nitrile nitrogen and aryl hydrogen of paired alkoxybenzonitriles (reproduction of Fig. 4), measured at the final state of MD simulations from ordered initial states. 1: ideal bond distance;[29] 2: ideal bond angle. b) Percentage of alkoxybenzonitriles by CH•••NC bond angle. Inset: Angle being measured. c) Percentage of alkoxybenzonitriles by CH•••NC distance. See Table S2 for sample size, simulation times, and statistical analysis.

Table S2. Most frequent bond distance and average bond angle of CH•••NC bonds, measured from MD simulations with an ordered initial state after the simulation time indicated. There is significant asymmetry in the distribution of bond lengths, so we report the position of the distribution maximum (mode function) with first and third quartiles as estimated error values. For the bond angles, averages are reported for bonds with distances less than 5.845 Å with one standard deviation reported as estimated error. The number of bonds counted in each case is reported as *N*.

	Most Frequent CH•••NC Bond Distance (Å)	Average CH•••NC Bond Angle (Degrees)	Time (ns) corresponding to measurements	*N*
ABN-C$_{18}$	2.7 (+ 0.3 / – 0.2)	116 (± 12)	368	98
ABN-C$_{12}$	2.9 (+ 0.1 / – 0.1)	117 (± 10)	285	160
ABN-C$_{8}$	2.7 (+ 0.7 / – 0.3)	121 (± 18)	354	152
ABN-C$_{4}$	2.8 (+ 0.3 / – 0.1)	119 (± 11)	326	223

Frequencies of Partial and Full Desorption Initiated by Benzonitrile Head and Alkyl Tail

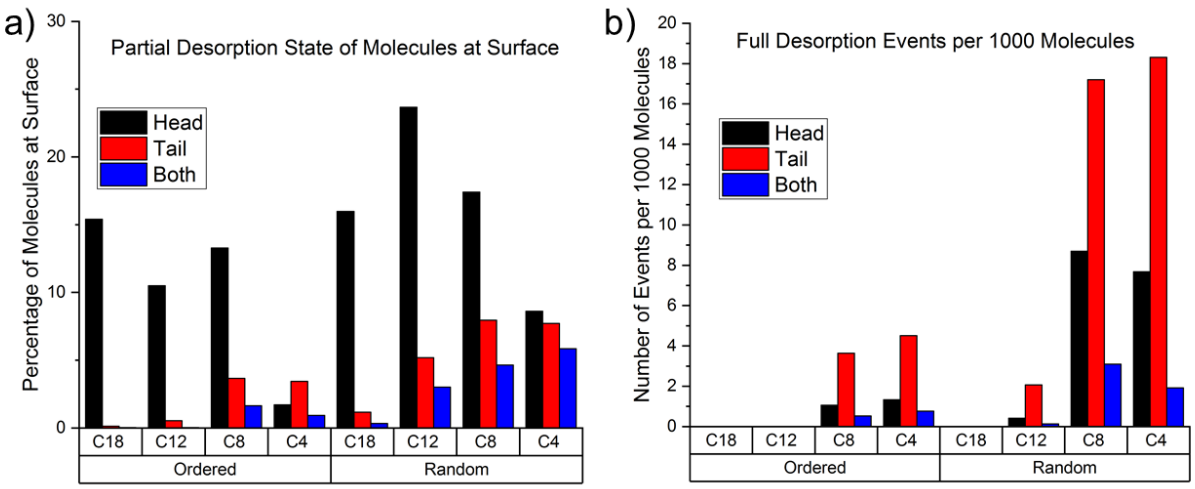

Figure S10. Analysis of MD results for (a) partial desorption events and (b) full desorption events for ABN molecules with four different alkyl chain lengths, each starting in an ordered or random initial state. (a) Percentage of molecules at the surface that have a partially desorbed benzonitrile head (black), partially desorbed alkyl tail (red), or both (blue). (b) Number of complete desorption events that originated from the head group (black), tail group (red), or both (blue). Data values for (a) are given in Table S3, along with the total number of molecules analyzed.

In considering the head group adsorption/desorption, it is important to consider that the CN group and benzene ring will move as a single rigid benzonitrile unit. When we compare a tail of comparable mass to the head group, C8, in a random initial configuration, we find that the head group undergoes a partial desorption event about twice as often as the tail (see Figure S10 and Table S3). These should have comparable interaction strengths to the surface, so this is most likely due to the flexible character of the tail compared to the head and to the interactions to neighboring adsorbates. When the same molecule is in the ordered initial state (better packing of molecules) the head group is in a partially desorbed state about 25% less often, but the tail partial desorption events drop by more than 50%. We note that when the tail is significantly longer (C18), the partial desorption events of the tail become much less frequent, especially for the ordered initial state.

Table S3. Percent of adsorbed alkoxybenzonitriles with partially desorbed benzonitrile groups (head), alkyl chains (tail), or both, obtained by analysis of snapshots from the MD simulations. Fully desorbed molecules were excluded from this analysis. The top part of the table is for simulations starting from the initially ordered state and the bottom section is for the random initial state. The bottom row of each section gives the total number of molecules included in the analysis for each molecule. Refer to "Simulation Analysis" section for further details about analysis.

	Initially Ordered State			
	ABN-C_{18}	**ABN-C_{12}**	**ABN-C_8**	**ABN-C_4**
% Desorbed head	15.4 %	10.5 %	13.3 %	1.7 %
% Desorbed tail	0.1 %	0.5 %	3.7 %	3.5 %
% Desorbed from both sides	< 0.1 %	< 0.1 %	1.7 %	0.9 %
% Molecules fully adsorbed	84.4 %	88.9 %	81.4 %	93.9 %
Total molecules in this analysis	13531	10931	15112	15730

	Initially Random State			
	ABN-C_{18}	**ABN-C_{12}**	**ABN-C_8**	**ABN-C_4**
% Desorbed head	16.0 %	23.7 %	17.4 %	8.6 %
% Desorbed tail	1.2 %	5.2 %	7.9 %	7.7 %
% Desorbed from both sides	0.3 %	3.0 %	4.6 %	5.8 %
% Molecules fully adsorbed	82.5 %	68.1 %	12.8 %	21.3 %
Total molecules in this analysis	8559	7238	5172	6770

Re-adsorption of Alkoxybenzonitriles from Solution Phase onto Adsorption onto HOPG

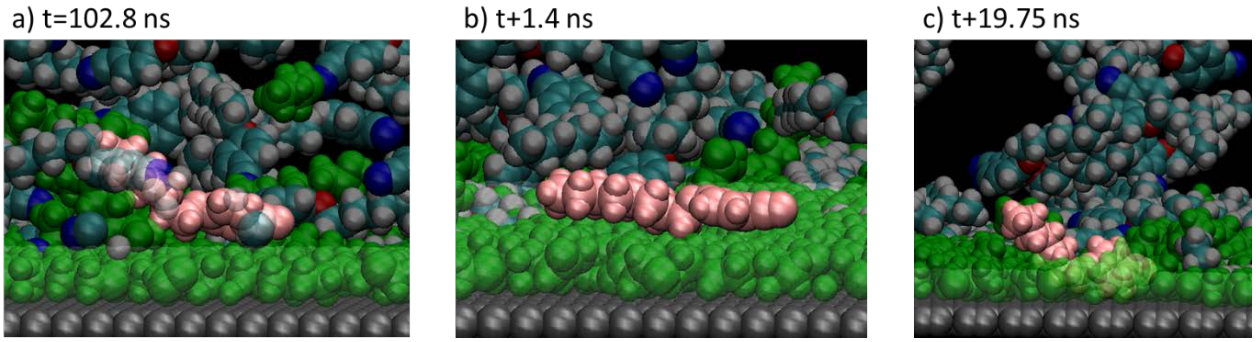

Figure S11. Re-adsorption of **ABN-C$_8$**. a) The benzonitrile group initiates adsorption onto the molecular monolayer. b) The entire alkoxybenzonitrile molecular peels onto the existing monolayer. c) The re-adsorbing alkoxybenzonitrile diffuses into the open graphite area.

References

1. J. Lee, S.-U. Kang, J.-O. Lim, H.-K. Choi, M.-k. Jin, A. Toth, L. V. Pearce, R. Tran, Y. Wang, T. Szabo and P. M. Blumberg, *Bioorg. Med. Chem.*, 2004, **12**, 371-385.
2. G. M. Fischer, M. Isomäki-Krondahl, I. Göttker-Schnetmann, E. Daltrozzo and A. Zumbusch, *Chem. Eur. J.*, 2009, **15**, 4857-4864.
3. S. Ahn, C. N. Morrison and A. J. Matzger, *J. Am. Chem. Soc.*, 2009, **131**, 7946-7947.
4. A. C. Vaiana, Z. Cournia, I. B. Costescu and J. C. Smith, *Comp. Phys. Commun.*, 2005, **167**, 34-42.
5. B. R. Brooks, C. L. Brooks, A. D. Mackerell, L. Nilsson, R. J. Petrella, B. Roux, Y. Won, G. Archontis, C. Bartels, S. Boresch, A. Caflisch, L. Caves, Q. Cui, A. R. Dinner, M. Feig, S. Fischer, J. Gao, M. Hodoscek, W. Im, K. Kuczera, T. Lazaridis, J. Ma, V. Ovchinnikov, E. Paci, R. W. Pastor, C. B. Post, J. Z. Pu, M. Schaefer, B. Tidor, R. M. Venable, H. L. Woodcock, X. Wu, W. Yang, D. M. York and M. Karplus, *J. Comput. Chem.*, 2009, **30**, 1545-1614.
6. V. Zoete, M. A. Cuendet, A. Grosdidier and O. Michielin, *J. Comput. Chem.*, 2011, **32**, 2359-2368.
7. K. Vanommeslaeghe, E. Hatcher, C. Acharya, S. Kundu, S. Zhong, J. Shim, E. Darian, O. Guvench, P. Lopes, I. Vorobyov and A. D. Mackerell, *J. Comput. Chem.*, 2010, **31**, 671-690.
8. A. D. Becke, *Phys. Rev. A*, 1988, **38**, 3098-3100.
9. A. D. Becke, *J. Chem. Phys.*, 1993, **98**, 5648-5652.
10. S. H. Vosko, L. Wilk and M. Nusair, *Canadian Journal of Physics*, 1980, **58**, 1200-1211.
11. C. Lee, W. Yang and R. G. Parr, *Phys. Rev. B*, 1988, **37**, 785-789.
12. P. J. Stephens, F. J. Devlin, C. F. Chabalowski and M. J. Frisch, *J. Phys. Chem.*, 1994, **98**, 11623-11627.
13. P. C. Hariharan and J. A. Pople, *Theoretica chimica acta*, 1973, **28**, 213-222.
14. Jaguar, version 8.1; Schrödinger, LLC: New York, 2013.
15. A. D. MacKerell, D. Bashford, M. Bellott, R. L. Dunbrack, J. D. Evanseck, M. J. Field, S. Fischer, J. Gao, H. Guo, S. Ha, D. Joseph-McCarthy, L. Kuchnir, K. Kuczera, F. T. K. Lau, C. Mattos, S. Michnick, T. Ngo, D. T. Nguyen, B. Prodhom, W. E. Reiher, B. Roux, M. Schlenkrich, J. C. Smith, R. Stote, J. Straub, M. Watanabe, J. Wiorkiewicz-Kuczera, D. Yin and M. Karplus, *J. Phys. Chem. B*, 1998, **102**, 3586-3616.
16. M. J. Frisch, G. W. Trucks, H. B. Schlegel, G. E. Scuseria, M. A. Robb, J. R. Cheeseman, G. Scalmani, V. Barone, B. Mennucci, G. A. Petersson, H. Nakatsuji, M. Caricato, X. Li, H. P. Hratchian, A. F. Izmaylov, J. Bloino, G. Zheng, J. L. Sonnenberg, M. Hada, M. Ehara, K. Toyota, R. Fukuda, J. Hasegawa, M. Ishida, T. Nakajima, Y. Honda, O. Kitao, H. Nakai, T. Vreven, J. Montgomery, J. A., J. E. Peralta, F. Ogliaro, M. Bearpark, J. J. Heyd, E. Brothers, K. N. Kudin, V. N. Staroverov, R. Kobayashi, J. Normand, K. Raghavachari, A. Rendell, J. C. Burant, S. S. Iyengar, J. Tomasi, M. Cossi, N. Rega, N. J. Millam, M. Klene, J. E. Knox, J. B. Cross, V. Bakken, C. Adamo, J. Jaramillo, R. Gomperts, R. E. Stratmann, O. Yazyev, A. J. Austin, R. Cammi, C. Pomelli, J. W. Ochterski, R. L. Martin, K. Morokuma, V. G. Zakrzewski, G. A. Voth, P. Salvador, J. J. Dannenberg, S. Dapprich, A. D. Daniels, Ö. Farkas, J. B. Foresman, J. V. Ortiz, J. Cioslowski and D. J. Fox, Gaussia09, Gaussian, Inc., Wallingford, Connecticut (2009).
17. C. Lee, W. Yang and R. G. Parr, *Phys. Rev. B*, 1988, **37**, 785-789.
18. S. H. Vosko, L. Wilk and M. Nusair, *Canadian Journal of Physics*, 1980, **58**, 1200-1211.

19. S. Grimme, J. Antony, S. Ehrlich and H. Krieg, *J. Chem. Phys.*, 2010, **132**, 154104.
20. G. Bussi, D. Donadio and M. Parrinello, *J. Chem. Phys.*, 2007, **126**, 014101.
21. W. G. Hoover, *Phys. Rev. A*, 1985, **31**, 1695-1697.
22. I. G. Tironi, R. Sperb, P. E. Smith and W. F. van Gunsteren, *J. Chem. Phys.*, 1995, **102**, 5451-5459.
23. B. Hess, H. Bekker, H. J. C. Berendsen and J. G. E. M. Fraaije, *J. Comput. Chem.*, 1997, **18**, 1463–1472.
24. S. Pronk, S. Páll, R. Schulz, P. Larsson, P. Bjelkmar, R. Apostolov, M. R. Shirts, J. C. Smith, P. M. Kasson, D. van der Spoel, B. Hess and E. Lindahl, *Bioinformatics*, 2013, **29**, 845-854.
25. W. Humphrey, A. Dalke and K. Schulten, *J. Mol. Graph.*, 1996, **14**, 33-38.
26. MATLAB, The MathWorks, Inc., Natick, Massachusetts.
27. D. G. Liakos and F. Neese, *J. Chem. Theory Comput.*, 2015, **11**, 2137-2143.
28. A. Goursot, T. Mineva, R. Kevorkyants and D. Talbi, *J. Chem. Theory Comput.*, 2007, **3**, 755-763.
29. G. R. Desiraju and T. Steiner, *The Weak Hydrogen Bond*, Oxford University Press, Oxford, 1999.